Radiofrequency Exposure induced by an Attocell of an Ultra-High Density Access Network

Günter Vermeeren[1], Arno Thielens[2], Olivier Caytan[3], Guy Torfs[3], Piet Demeester[3], Johan Bauwelinck[3], Hendrik Rogier[3], Luc Martens[1], and Wout Joseph[2]

[1] WAVES, imec / Ghent University, Ghent, Belgium

[2] WAVES, Ghent University, Ghent, Belgium

[3] IBCN, Ghent University, Ghent, Belgium

[*]Corresponding author e-mail: Gunter.Vermeeren@UGent.be

SHORT ABSTRACT

We evaluated the exposure induced by an attocell of an ultra-high density access network radiating at 3.5 GHz with an antenna input power of 1 mW. We simulated and measured incident field exposure and absorption induced by the antenna of a single cell in a flat phantom and assessed the absorption in a realistic human body model. All measured and simulated E_{RMS} values above the attocell were below 5.9 V/m. The SAR_{10g} values were measured in a homogeneous phantom, which resulted in a SAR_{10g} of 9.7 mW/kg, and using FDTD simulations, which resulted in a SAR10g of 7.2 mW/kg. Simulations of realistic exposure of a heterogeneous phantom yielded SAR_{10g} values below 2.8 mW/kg. The studied dosimetric quantities are compliant with the ICNIRP guidelines.

INTRODUCTION

It is expected that in future 5th generation networks, the required bandwidth and data throughput will increase [1]. A potential approach to deal with this increase in demands from the network is to deploy an ultra-high density access network consisting of large number of very small cells, so called attocells [2]. An attocell is a cell which is integrated in a floor and cover very small areas of only a few dm². Yet, they provide a very high data rate in these small areas. Since attocells will be smaller and widely distributed in indoor environments, the antennas used in attocells will be closer to the user than those employed in previous generations of cellular networks [3]. This close distance might be a risk in terms of personal exposure to the RF EMFs emitted by the antennas.

The objective of this paper is to study the RF exposure near an attocell. To this aim both measurements near an actual attocell configuration and numerical simulations of a model of the same attocell are executed. First, the E_{RMS} field strengths are studied near the attocell in its worst-case operating conditions. Second, the peak SAR_{10g} is studied in a standardized phantom near the antenna used in the attocell. Third, the realistic SAR_{10g} in a heterogeneous phantom is studied near the attocell. These results are important for the implementation of 5th generation networks, which require a compliance with EMF standards.

MATERIALS AND METHODS

Figure 1 shows an illustration of the implementation of the attocells in a transparent floor. A layer of acrylic glass (thickness = 6 mm) was supported by a wooden framework that maked up the different attocells. Each cell is 15 x 15 cm² and contained an antenna that operated between 3.25 GHz and 3.75 GHz. The antennas are linearly polarized planar, substrate-integrated-waveguide (SIW) cavity-backed slot antennas, made out of foam material (the substrate) and copper plated nylon (the conducting elements) [4]. The communication protocol of the attocell applied a maximum input power of 1 mW at the feed point of the antennas at a center frequency of 3.5 GHz in a frequency band between 3.25 GHz and 3.75 GHz. This

frequency band was chosen because it is located in the lower part of the Ultra-Wide Band (UWB), which ranges from 3.1 GHz to 10.6 GHz [5].

Figure 1: 3x3 attocells implemented in a transparent floor.

The EMF measurements near the attocells were performed using a DASY3 mini system (SPEAG, Zurich, Switzerland). The system consisted of two parts. First, an isotropic E-Field Probe for general near-field measurements (ER3DV6, SPEAG, Switzerland), which was able to measure in a frequency range of 40 MHz - 6 GHz had a dynamic range of 2-1000 V/m, and a linearity of ±0.2 dB. The second component of the system was a Pythron IXE α-C-T robot, which enabled a three-dimensional translation of the probe with an accuracy of 0.005 mm. The total expanded uncertainty (k=2) of the setup for free-space near-field measurements was 14 %, based on the DASY3 mini application note [6]. The antenna in the attocell was excited by a sinusoidal wave from a signal generator (SMB 100A, Rhode & Schwartz, Munich, Germany) with a power of 16 dBm and rescaled to an antenna input power of 0 dBm (1 mW) at 3.5 GHz. The field probe was used to scan an area of 30 cm in the X-direction and 30 cm in the Y-direction (corresponding to 4 attocells) with a step size of 15 mm resulting in a total of 441 points in the horizontal plane, at different separation distances in the Z-direction from the antenna. During the measurements the separation distance was defined as the distance to the top of the antenna, which was placed in one of the four attocells. Measurements were performed at distances 70 mm, 100 mm and 120 mm.

For the SAR compliance assessment, again the DASY 3 mini system (SPEAG, Switzerland) was used in combination with the isotropic dosimetric probe EX3DV4 (SPEAG, Switzerland). One antenna was detached from the setup and placed underneath a standardized oval flat phantom (ELI4, SPEAG, Zurich, Switzerland) compatible with the IEC 62209-2 standard. This phantom was filled with tissue simulating liquid HSL2450 (SPEAG, Switzerland) used at 3.5 GHz with a measured relative permittivity ε_r= 36.1 and conductivity σ= 2.47 S/m. The patch of the antenna was facing upwards towards the flat surface of the phantom at a distance of 10 mm from the tissue simulating liquid.

For the investigation of the SAR in the realistic human body model, we selected Duke, the 34-year-old adult male from the Virtual Population [7] with a mass of 72.2 kg and a height of 1.80 m. The dielectric properties of the phantom were loaded from the database included in Sim4life, which was based on [8]. The phantom has a mass of 72.2 kg, which implies that its SAR_{wb} can never be higher than 0.08 W/kg (ICNIRP basic restriction for general public [9]) for an input power of 1 mW. Therefore, only the peak SAR_{10g} was studied for the heterogeneous phantom.

RESULTS

Figure 2(a) shows the results of electric field strength measurements at a separation distance of 8 mm above the acrylic glass, which corresponds to a distance of 7 cm above the antenna (the closest area scan performed to the antenna), while the antenna is fed with an input power of 1 mW at 3.5 GHz. The maximum E_{RMS} value in the plane is 5.9 V/m.

Figure 2(b) shows the measured SAR in the flat phantom at 5 mm from the phantom's shell inside the liquid for the attocell whose antenna receives an input power of 1 mW at 3.5 GHz. The distance of 5 mm is in compliance with the IEC 62209-2 standard for the area scan [10]. The measured peak SAR_{10g} equaled 9.7 mW/kg. This value is about 200 times smaller than the ICNIRP basic restriction of 2W/kg on the SAR_{10g}.

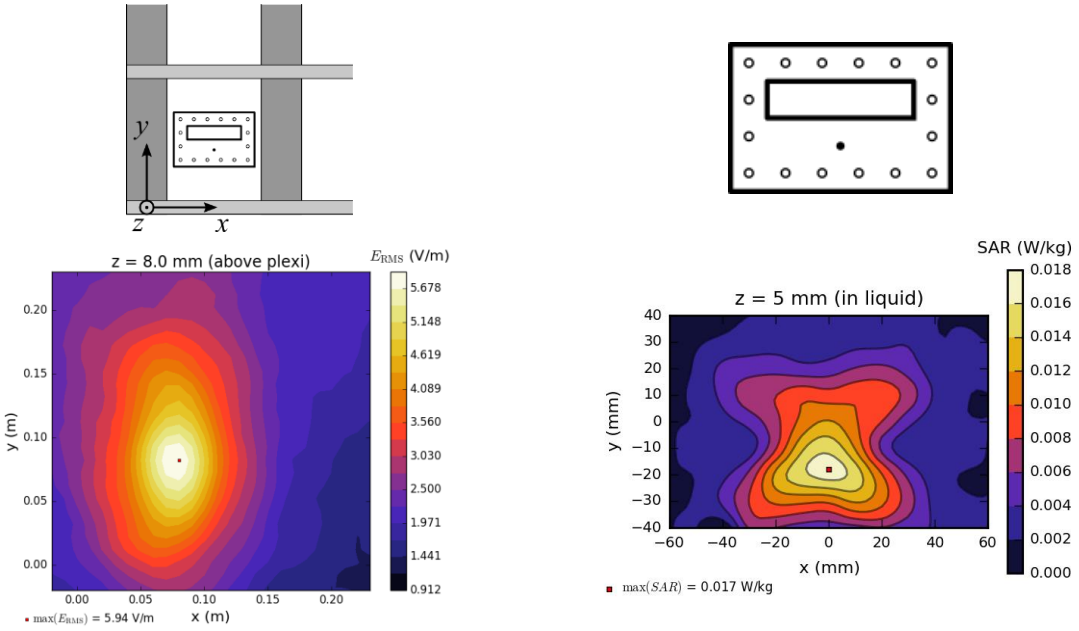

(a) (b)

Figure 2: (a) Electric field (E_{RMS}) at 8 mm above the acrylic glass for the attocell and (b) SAR measurements at 5 mm from the phantom's inner shell using for an input power of 1 mW at 3.5 GHz.

We assessed numerically the localized peak SAR_{10g} for the six different configurations shown in Figure 3 and compared it to the ICNIRP basic restrictions on the peak SAR10g for the general public, which are 2 W/kg for the head and trunk and 4 W/kg in the limbs. Table 1 lists the peak SAR_{10g} values obtained from the FDTD simulations, normalized to an input power of 1 mW. All values are far below the ICNIRP basic restrictions on peak SAR_{10g}.

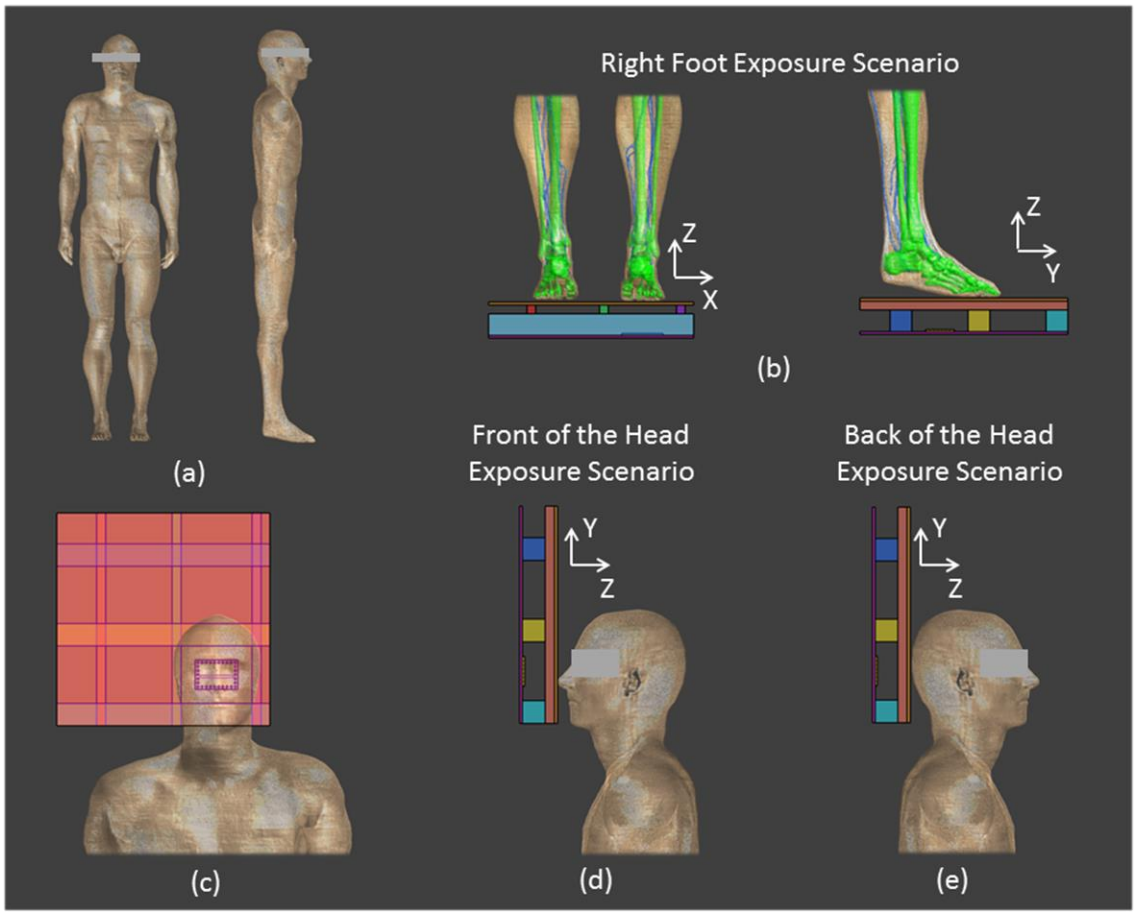

Figure 3: Configuration of the FDTD simulations. (a) Duke in a frontal and side view. (b) Placement of the attocell underneath the right foot of Duke. The skin of the foot touches the layer of acrylic glass. (c) Alignment of Duke's head with the attocell. (d) Duke's head placed in front of the attocell, facing the attocell. (e) Duke's head placed in front of the attocell, facing the opposite direction.

Table 1: Peak SAR10g values (in W/kg) in the VFM, normalized to an input power of 0 dBm in the attocell for six different configurations (three positions with respect to the human body and two orientations of the antenna).

	Back of the head		**Front of the head**		**Right Foot**	
Antenna orientation	Horizontal	Vertical	Horizontal	Vertical	Horizontal	Vertical
peak SAR_{10g} (mW/kg)	1.86	2.09	2.80	2.28	1.21	1.38

CONCLUSIONS

This study investigated the exposure induced by an attocell operating at 3.5 GHz with an input power of 1 mW in terms of RF EM fields and SAR. The RMS electric field equaled 5.9 V/m and complied with ICNIRP reference levels. A SAR compliance assessment of the antenna deployed in the attocell is executed according to the IEC 62209-2 standard, which resulted in peak SAR_{10g} values of 9.7 mW/kg obtained by measurements. These are far below (about a factor 200) the basic restriction for the general public issued by ICNIRP. The compliance assessment is then complimented by FDTD simulations on a realistic, heterogeneous model in

six real-life situations. The simulations result in peak SAR_{10g} values that are smaller than 2.8 mW/kg. This is more than a factor of 290 smaller than the relevant basic restrictions for the general public at 3.5 GHz. We conclude that attocells are an interesting solution to provide high-bandwidth coverage, while maintaining a low exposure to RF EM fields for the users.

REFERENCES

[1] The 5G Infrastructure Public Private Partnership (5GPP). 2014. 5G Vision: the next generation of communication networks and services. White paper. Available from: https://5g-ppp.eu/wp-content/uploads/2015/02/5G-Vision-Brochure-v1.pdf [Last accessed 20 September 2016].

[2] Lannoo B, Dixit A, Colle D, Bauwelinck J, Dhoedt B, Jooris B, Moerman I, Pickavet M, Rogier H, Simoens P, Torfs G, Vande Ginste D, and Demeester P. 2015. Radio-over-Fibre for Ultra-Small 5G Cells. 17th International Conference on Transparent Optical Networks (ICTON). 5-9 July 2015, Budapest, Hungary.

[3] Gupta A, and Kumar RJHA. 2015. A Survey of 5G Network: Architecture and Emerging Technologies. IEEE Access 3:1206–1232.

[4] Lemey S, Declerq F, and Rogier H. 2014. Dual-band substrate integrated waveguide textile antenna with integrated solar harvester. IEEE Antennas and Wireless Propagation Letters 13:269-272.

[5] Porcino D, and Hirt W. 2003. Ultra-Wideband Radio Technology: Potential and Challenges Ahead. IEEE Communications Magazine 41 (7):66-74.

[6] SPEAG. DASY 3 measurement system - Application Note: System Description and Setup. Zurich, Switzerland.

[7] Christ A, Kainz W, Hahn EG, Honegger K, Zefferer M, Neufeld E, Rascher W, Janka R, Bautz W, Chen J, Kiefer B, Schmitt P, Hollenbach H, Shen J, Oberle M, Szczerba D, Kam A, Guag JW, Kuster N. 2010. The Virtual Family, development of surface-based anatomical models of two adults and two children for dosimetric simulations. Phys Med Biol 55:N23-38.

[8] Gabriel S, Lau RW, Gabriel C. 1996. The dielectric properties of biological tissues: III. Parametric models for the dielectric spectrum of tissues. Phys Med Biol 41:2271-2293.

[9] International Comission on Non-Ionizing Radiation Protection, 1998. Guidelines for limiting exposure to time-varying electric, magnetic, and electromagnetic fields (up to 300 GHz). Health physics, 74(4), pp.494–522.

[10] International Electrotechnical Commission, 2010. IEC 62209-2 ed. 1: Human exposure to radio frequency fields from hand-held and body-mounted wireless communication devices – Human models, instrumentation, and procedures – Part 2: Procedure to determine the specific absorption rate (SAR) for wireless communication.